

Article

MW-Promoted Cu(I)-Catalyzed P–C Coupling Reactions without the Addition of Conventional Ligands; an Experimental and a Theoretical Study

Bianka Huszár, Réka Henyecz, Zoltán Mucsi and György Keglevich * 

Department of Organic Chemistry and Technology, Budapest University of Technology and Economics, 1521 Budapest, Hungary; huszar.bianka@vbk.bme.hu (B.H.); reka422@gmail.com (R.H.); zoltanmucsi@gmail.com (Z.M.)

* Correspondence: keglevich.gyorgy@vbk.bme.hu; Tel.: +36-1-463-1111 (ext. 5883)

Abstract: An experimental and a theoretical study on the so far less investigated Cu(I) salt-catalyzed Hirao reaction of iodobenzene and diarylphosphine oxides (DAPOs) revealed that Cu(I)Br or Cu(I)Cl is the most efficient catalyst under microwave irradiation. The optimum conditions included 165 °C and a 1:2 molar ratio for DAPOs and triethylamine. The possible ligations of Cu(I) were studied in detail. Bisligated P–Cu(I)–P (A), P–Cu(I)–N (B) and N–Cu(I)–N (C) complexes were considered as the catalysts. Calculations on the mechanism suggested that complexes A and B may catalyze the P–C coupling, but the latter one is more advantageous both according to experiments and calculations pointing out the Cu(I) → Cu(III) conversion in the oxidative addition step. The P–C coupling cannot take place with PhBr, as in this case, the catalyst complex cannot be regenerated.



Citation: Huszár, B.; Henyecz, R.; Mucsi, Z.; Keglevich, G. MW-Promoted Cu(I)-Catalyzed P–C Coupling Reactions without the Addition of Conventional Ligands; an Experimental and a Theoretical Study. *Catalysts* **2021**, *11*, 933. <https://doi.org/10.3390/catal11080933>

Academic Editors: Giuseppe Bagnato and Fausto Gallucci

Received: 13 July 2021

Accepted: 28 July 2021

Published: 30 July 2021

Publisher's Note: MDPI stays neutral with regard to jurisdictional claims in published maps and institutional affiliations.



Copyright: © 2021 by the authors. Licensee MDPI, Basel, Switzerland. This article is an open access article distributed under the terms and conditions of the Creative Commons Attribution (CC BY) license (<https://creativecommons.org/licenses/by/4.0/>).

Keywords: Hirao reaction; copper(I) catalyst; microwave; tertiary phosphine oxide; theoretical calculations; ligation; mechanism; Cu(I) → Cu(III) transition

1. Introduction

The Hirao reaction belongs to the large family of metal catalyzed cross-couplings [1–5]. Originally Pd(PPh₃)₄ was applied as the catalyst in the reaction of vinyl- or aryl bromides and dialkyl phosphites [1,2]. Later on, Pd or Ni salts (e.g., Pd(OAc)₂ and NiCl₂) were used as the precursor of metals together with mono- and bidentate P-ligands and the reaction was extended to other model compounds [3–5]. Keglevich and co-workers elaborated a microwave (MW)-assisted Pd or Ni-catalyzed P–C coupling, where the excess of the >P(O)H reagent served, via its trivalent tautomeric form (>POH) as the P-ligand [6–8]. Intensive studies involving experiments and calculations explored the fine mechanism of the Pd- and Ni-catalyzed variations. In contrast to the Pd(II) → Pd(0) conversion [9,10] observed for the Pd(OAc)₂-catalyzed option, a Ni(II) → Ni(IV) transition was substantiated for the NiCl₂-promoted case [11,12]. This was a brand new observation [13].

Cu-catalysis offers cheaper and hence a more practical realization of P–C coupling reactions as compared to the use of Pd- or Ni-catalysts, but this option has only been studied occasionally. The first Cu-catalyzed Hirao reaction of aryl halides and dibutyl phosphite using CuI as the precursor was carried out by Buchwald et al. [14]. During the syntheses, DMEDA proved to be a useful N-ligand, that was also applied in further cases [15–17]. Other N-ligands were also tested in the “CuI-catalyzed” coupling reactions: Beletskaya et al. found 2,2'-bipyridine and 1,10-phenanthroline to be the best ligands in the reaction of aryl iodides and diethyl phosphite, but good results were obtained in the presence of TMEDA, 1-methyl-1*H*-imidazole [18], *N*-methylpyrrolidine-2-carboxamide [19], proline and pipercolic acid [20], (*S*)- α -phenylethylamine [21,22], or 1-pyrroldinylphosphonic acid monophenyl ester as well [23]. It is noted that the reactivity of aryl bromides was far behind that of the corresponding iodides, but when the bromoarenes were pre-reacted with

potassium iodide, the yields could be increased with ca. 50% [20,23]. Arylboronic acids were also suitable substrates for phosphonylation with dialkyl phosphites in the presence of Cu_2O as the catalyst precursor and 1,10-phenanthroline as the ligand [24]. Until now, only two “ligand-free” Cu-catalyzed P–C coupling reactions have been described. In the first case, vinyl phosphonates were obtained applying a large excess of CuI and NEt_3 or KH [25]. Later on, aryl halides with an *ortho*-hydroxy group were reacted with $>\text{P}(\text{O})\text{H}$ compounds in the presence of CuI and Cs_2CO_3 [26].

One can see that almost all Cu-catalyzed P–C couplings were performed in the presence of N-ligands and the activity of Cu was lower as compared to the Pd- or Ni-catalysts. Due to the several possible oxidation states of Cu, the mechanism of the transformations described above is presumably complex and for this, it has not yet been studied in detail.

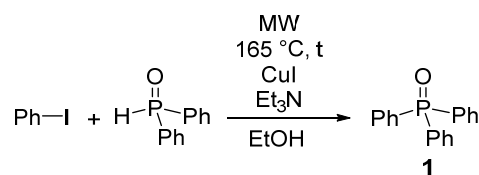
In this work, the results of the Cu(I) salt-catalyzed P–C coupling reactions of secondary phosphine oxides and iodobenzene obtained experimentally and by quantum chemical calculations are summarized.

2. Results and Discussion

2.1. Experimental Results on the Hirao Reaction of Iodobenzene and Diarylphosphine Oxides

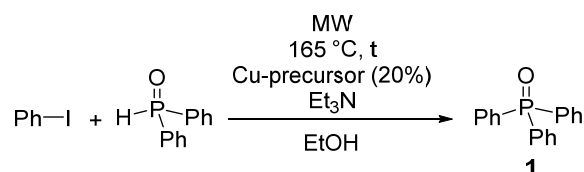
It is well-known from earlier studies that the Cu^+ -catalysis is less efficient than the Pd- or Ni-promoted cases. To compensate the lower reactivity of the Cu^+ -catalyst, the more reactive iodobenzene was selected as the reactant with diphenylphosphine oxide under MW-assisted conditions. The first set of P–C couplings was carried out using CuI as the catalyst and triethylamine as the base in ethanol as the medium at a temperature of 165 °C (Table 1). In the absence of catalyst, there was practically no reaction (Table 1/Entry 1). Using 10% of CuI and 1 equivalent of each of $\text{Ph}_2\text{P}(\text{O})\text{H}$ and NEt_3 , the conversion was 44% after a 3 h of irradiation (Table 1/Entry 2). Offering a 20% excess of $\text{Ph}_2\text{P}(\text{O})\text{H}$ to act as a P-ligand, the conversion decreased to 35% (Table 1/Entry 3). At the same time, measuring in 2 equivalents of TEA, the conversion increased to 51% (Table 1/Entry 4) meaning that Cu^+ may prefer TEA to $\text{Ph}_2\text{P}(\text{O})\text{H}$ as the ligand. The P–C couplings became somewhat more efficient, when 20% of the catalyst was applied. The tendencies were the same: the use of 40% excess of $\text{Ph}_2\text{P}(\text{O})\text{H}$ was not advantageous (Table 1/Entry 7). At the same time, applying NEt_3 in a 2 equivalents' quantity, the conversion increased to 63% (Table 1/Entry 8). Extension of the reaction time to 4 h was useful, as conversions of 61 and 75% could be attained as compared to the 3 h expositions (Table 1/Entries 6 and 9 vs. entries 5 and 8). It is noteworthy that the formation of $\text{Ph}_2(\text{EtO})\text{P}(\text{O})$ as a side-product ($\delta_{\text{P}}(\text{CDCl}_3)$ 31.5, $[\text{M} + \text{H}]^+_{\text{found}} = 247.0882$, $\text{C}_{14}\text{H}_{16}\text{O}_2\text{P}$ requires 247.0888) was inevitable during the coupling reactions by the participation of the solvent. Its quantity fell in the range of 1–7%.

In the next stage, different Cu^+ precursors were tested in the model reaction selected. Applying 20% of CuBr as the catalyst at 165 °C for 3 h at a 1:1 ratio of $\text{Ph}_2\text{P}(\text{O})\text{H}$ and NEt_3 , the conversion was 75% (Table 2/Entry 2). Using 1.4 equivalents of the P-reagent, the conversion dropped to 50% (Table 2/Entry 3). However, when the quantity of NEt_3 was increased to two equivalents, a higher conversion of 90% was attained (Table 2/Entry 4). Triphenylphosphine oxide (1) was obtained in 65 and 85% yields from the better experiments (Table 2/Entries 2 and 4). One can see that in the P–C coupling reaction under discussion, CuBr is a more efficient catalyst than CuI.

Table 1. Optimization of the P–C coupling reaction of iodobenzene and diphenylphosphine oxide in the presence of CuI.

Entry	CuI (%)	DPPO (equiv.)	NEt ₃ (equiv.)	t (h)	Conversion (%) ^{a,b}	Yield (%) ^b
1	-	1	1	4	3	-
2	10	1	1	3	44 ^{c,d}	-
3	10	1.2	1	3	35 ^c	-
4	10	1	2	3	51 ^c	-
5	20	1	1	3	52 ^c	-
6	20	1	1	4	61 ^c	51 (1)
7	20	1.4	1	3	50 ^c	-
8	20	1	2	3	63 ^c	64 (1)
9	20	1	2	4	75 ^c	68 (1)

^a Based on ³¹P NMR; ^b The average of two parallel experiments; ^c 1–7% Ph₂(EtO)P(O) was detected as a side-product. ^d Measuring in 1 equiv. of KI as an additive did not led to better result.

Table 2. Testing different Cu-precursors in the Hirao reaction of iodobenzene and diphenylphosphine oxide.

Entry	Cu-Precursor	DPPO (equiv.)	NEt ₃ (equiv.)	t (h)	Conversion (%) ^a	Yield (%)
1	CuI	1	2	4	75 ^{b,c}	68 (1)
2	CuBr	1	1	3	75 ^c	65 (1)
3	CuBr	1.4	1	3	50 ^c	-
4	CuBr	1	2	3	90 ^c	85 (1)
5	CuCl	1	1	3	71 ^c	60 (1)
6	CuCl	1.4	1	3	47 ^c	-
7	CuCl	1	2	3	84 ^{b,c}	78 (1)
8	CuCl	1	2	4	88 ^{b,c}	71 (1)

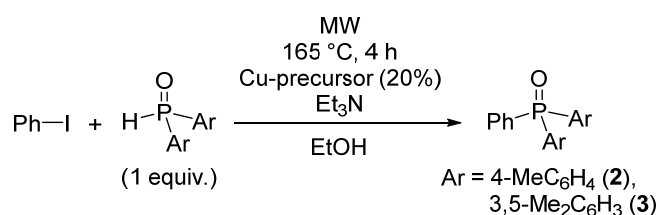
^a Based on ³¹P NMR; ^b The average of two parallel experiments; ^c Ph₂(EtO)P(O) was detected as a side-product.

Then, CuCl was applied as the catalyst precursor. The tendencies observed were similar experienced with CuBr, but the conversions were somewhat lower. Applying Ph₂P(O)H and the base in a one equivalent quantity, the conversion was 71% as compared to 75% (Table 2/Entry 5 vs. entry 2). Increasing the quantity of the P-reagent to 1.4 equivalents, the conversion was 47% against the value of 50% (Table 2/Entry 6 vs. entry 3). When NEt₃ was used in an excess (two equivalents), a conversion of 84% was observed that was somewhat lower than the value of 90% obtained with CuBr (Table 2/Entry 7 vs. entry 4). A longer reaction time of 4 h led to a conversion of 88% (Table 2/Entry 8).

In conclusion, the higher conversions around 89% belonging to CuBr and CuCl catalyst precursors were obtained using two equivalents of NEt₃. One may see that CuBr was found the most efficient catalyst precursor in the series investigated. On the other hand, it may be observed from the experimental data that probably not the P–Cu(I)–P (A) complex is the active species, but rather the P–Cu(I)–N (B) or the N–Cu(I)–N (C) complex. The mixed ligation may be more realistic, as in this case, the reacting P moiety is also included. This problem will be discussed in the theoretical part, see Section 2.4.2.)

Bis(4-methylphenyl)phosphine oxide and bis(3,5-dimethylphenyl)phosphine oxide were also tested in the P–C coupling reactions applying Cu salt catalyst precursors (20%) at 165 °C in EtOH as the solvent. Applying CuCl in reaction with the 4-MePh derivative, it was better to use 2 equivalents of NEt₃ as compared to the case with only 1 equivalent of the amine, as marked by the conversions of 80% and 68%, respectively (Table 3/Entries 2 and 1). In the presence of CuBr, the conversion was better (83%) (Table 3/Entry 3).

Table 3. Extensions of the Cu-catalyzed P–C coupling reaction to substituted diarylphosphine oxides.



Entry	Ar	Cu-Precursor	NEt ₃ (equiv.)	Conversion (%) ^{a,b}	Yield (%)
1	4-MeC ₆ H ₄	CuCl	1	68 ^c	-
2	4-MeC ₆ H ₄	CuCl	2	80 ^c	71 (2)
3	4-MeC ₆ H ₄	CuBr	2	83 ^c	78 (2)
4	3,5-Me ₂ C ₆ H ₃	CuCl	1	77 ^d	-
5	3,5-Me ₂ C ₆ H ₃	CuCl	2	87 ^d	81 (3)
6	3,5-Me ₂ C ₆ H ₃	CuBr	2	90 ^d	84 (3)

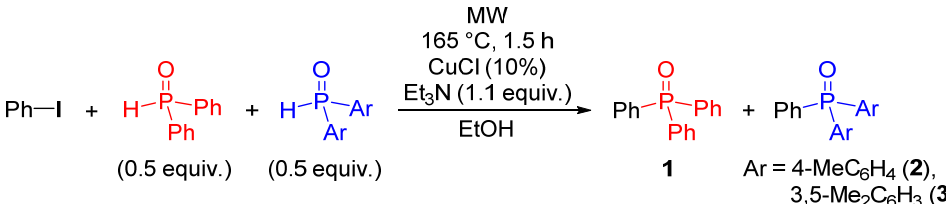
^a Based on ³¹P NMR; ^b The average of two parallel experiments; ^c (4-MeC₆H₄)₃P(O) was detected as a side-product; (δ_P(CDCl₃) 29.9, δ_P [27] (CDCl₃) 29.4; [M + H]⁺_{found} = 321.1401, C₂₁H₂₁OP requires 321.1408; ^d (3,5-diMeC₆H₃)₃P(O) was detected as a side-product; δ_P(CDCl₃) 30.2, δ_P [28] (CDCl₃) 30.9; [M + H]⁺_{found} = 363.1878 C₂₄H₂₇OP requires 363.1878.

Applying bis(3,5-dimethylphenyl)phosphine oxide as the P-reagent and ligand, somewhat higher (77, 87 and 90%) conversions were detected under the conditions applied above. (Compare entries 1 and 4, entries 2 and 5, as well as entries 3 and 6 of Table 3). Although appearance of the methyl group in position 4 of the phenyl ring slightly decreases the reactivity of the secondary phosphine oxide in the P–C coupling reaction under discussion, the steric hindrance due to the methyl groups may increase the activity of the catalyst formed, as in this case, bis-ligation is preferred [10]. After purification, diaryl-phenylphosphine oxides 2 and 3 were obtained in yields of 78% and 84%, respectively.

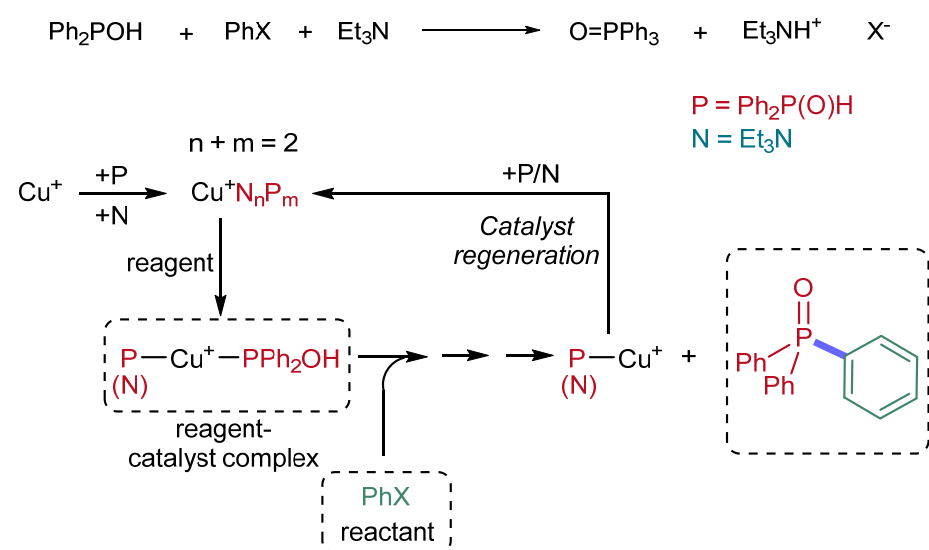
It can be seen that the methyl substitution in the phenyl ring is somewhat disadvantageous in the Hirao reaction. In order to prove this directly, competitive P–C couplings were carried out applying a 1:1 mixture of Ph₂P(O)H and Ar₂P(O)H in reaction with iodobenzene. The interrupted reactions revealed a 20:12 and a 23:15 ratio of Ph₃P(O) (1)–(4-MePh)₂P(O) (2) and Ph₃P(O) (1)–(3,5-diMePh)₂P(O) (3), respectively (Table 4/Entries 1 and 2), meaning that the secondary phosphine oxide is more reactive with phenyl groups than with 4-MePh and 3,5-diMePh substituents. The methyl group in position 4 results in larger electron density on the P atom increasing its complexation ability; at the same time, this substituent also results in a decrease in the acidity. In overall, the reactivity decreases. It was found earlier that both electron-donating and electron-withdrawing substituents decrease the reactivity of the bromoarene in P–C coupling reactions [7].

2.2. Theoretical Calculations

The computation study on the mechanism and on the energetics was carried out by the DFT method including the implicit solvent model [M06-2X/6-31G(d,p)//PCM(THF)]. The coupling of Ph₂P(O)H and halobenzenes in the presence of Cu⁺ catalyst served as the model reaction in our calculations. The sketch for the Cu⁺-catalyzed process is shown in Figure 1. In the first approach, both P- and N-ligation should be assumed, as they are competitive ligands to Cu⁺.

Table 4. Comparison of the reactivity of the diarylphosphine oxides in the Cu-catalyzed Hirao reaction.


Entry	Ar	Conversion (%) ^a	Composition (%) ^a	
			Ph ₃ P(O)	PhAr ₂ P(O)
1	4-MeC ₆ H ₄	36	20 (1)	12 (2)
2	3,5-Me ₂ C ₆ H ₃	39	23 (1)	15 (3)

^a Based on ³¹P NMR.**Figure 1.** General overview and the sequential steps of the catalytic P–C coupling.

From thermodynamic point of view, the overall reaction is exothermic for the two cases involving Br or I as the halogen substituent (Table 5). The coupling with PhI is more exothermic due to the higher stability of the I[−] in solution.

Table 5. The total enthalpy, Gibbs free energy (ΔH and ΔG in kJ mol^{−1}) and entropy (ΔS in J mol^{−1} K^{−1}) change of the Hirao reaction of Ph₂P(O)H with PhX.

Total Change In	ΔH	ΔG	ΔS
PhBr	−65.7	−47.4	−61.3
PhI	−155.4	−136.0	−65.3

The reaction unifies three main processes, such as the complexation, oxidative addition of the PhX reactant and finally the reductive elimination from the central metal ion (Figure 1). The catalyst is regenerated in the final stage of the reaction.

2.3. Complexation

The complexation process is rather complicated, as Cu⁺ may be ligated with both the tautomeric form of the reagent (Ph₂POH, **1a**) and the trialkylamine that is present as base. There is a multiple possibility for the formation of “Cu⁺P₄”, “Cu⁺N₄” and the mixed complexes as well. At first, examining only the “homogeneous” complexation, a series of P- and N-ligands were considered up to four ligations. For P-ligation, the complex formation

is beneficial in all steps up to the fourth ligation. However, the step-by-step enthalpy values are somewhat decreasing in the order of ligation(s) marked by numbers 1, 2, 3, 4. This is in contrast to the analogous complexation with Pd(0), where due to steric hindrance, the fourth ligation is already unfavorable. It means that despite the steric hindrance, the most preferred form for Cu⁺ is the tetra-coordinated complex. Even triphenylphosphine may be involved in tetracoordination as shown in Figure 2. In case of N-ligation, the sterically less hindered NMe₃ may participate in tetraligation, but the sterically more requiring NEt₃ and N^{*i*}Pr₃ may be involved in only triple- and bisligation, respectively. The computed values are summarized in Table 6 and visually displayed in Figure 2. According to the computed data, the N-ligation is stronger in the first two steps (1 and 2), but at higher coordinations (such as 3 and 4), the P-ligation overcomes N-ligation.

Table 6. Stepwise and accumulated complexation enthalpies (ΔH ; kJ mol⁻¹), Gibbs free energies (ΔG ; kJ mol⁻¹) for the Cu⁺ ion by P- and N-ligands listed in the first column assuming homogeneous complexation.

L	A		B		C		D		
	ΔH	ΔG							
Ph ₃ P	step	-274.0	-244.8	-191.2	-137.9	-170.5	-100.5	-82.1	-15.8
	Sum	-274.0	-244.8	-465.1	-382.7	-635.6	-483.1	-717.7	-498.9
Ph ₂ PHO	step	-257.8	-221.0	-180.6	-124.4	-146.0	-84.6	-130.4	-64.9
	Sum	-257.8	-221.0	-438.5	-345.4	-584.5	-430.0	-715.0	-494.9
<i>p</i> Tol ₂ PHO	step	-259.9	-225.1	-190.0	-111.8	-139.0	-0.9	-148.0	-68.8
	Sum	-259.9	-225.1	-449.9	-336.9	-588.9	-397.8	-736.9	-466.6
(3,5-diMePh) ₂ PHO	step	-269.5	-229.4	-208.1	-127.5	-144.0	-65.8	-172.2	-91.3
	Sum	-269.5	-229.4	-477.7	-356.9	-621.7	-422.7	-793.9	-514.0
Me ₃ N	step	-264.3	-230.9	-226.1	-171.4	-74.2	-24.3	-60.5	-3.2
	Sum	-264.3	-230.9	-490.4	-402.3	-564.6	-426.6	-625.1	-429.8
NEt ₃	step	-306.5	-266.8	-224.7	-165.9	-41.6	-20.2	-	-
	Sum	-306.5	-266.8	-531.2	-432.7	-572.8	-412.5	-	-
<i>i</i> Pr ₂ EtN	step	-307.4	-272.2	-243.7	-184.7	-	-	-	-
	Sum	-307.4	-272.2	-551.1	-456.9	-	-	-	-

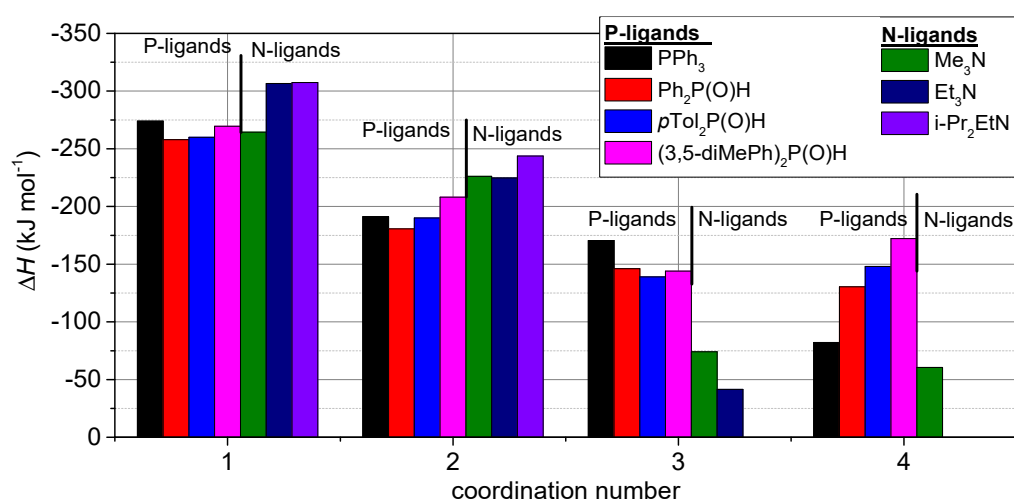


Figure 2. Enthalpy values (ΔH ; in kJ mol⁻¹) for the stepwise complexation of the Cu⁺ ion by P- and N-ligands.

Extending the study to “heterogeneous” complexation, where NEt_3 and $\text{Ph}_2\text{P}(\text{O})\text{H}$ are present at the same time and compete with each other; overall, 14 species may be deduced. The map of the possible complexations is presented in Figure 3 together with the stepwise enthalpies computed. Figure 4 summarizes the situation showing that in case of higher ligations, the complexation with P-ligands is more beneficial than that with N-ligands.

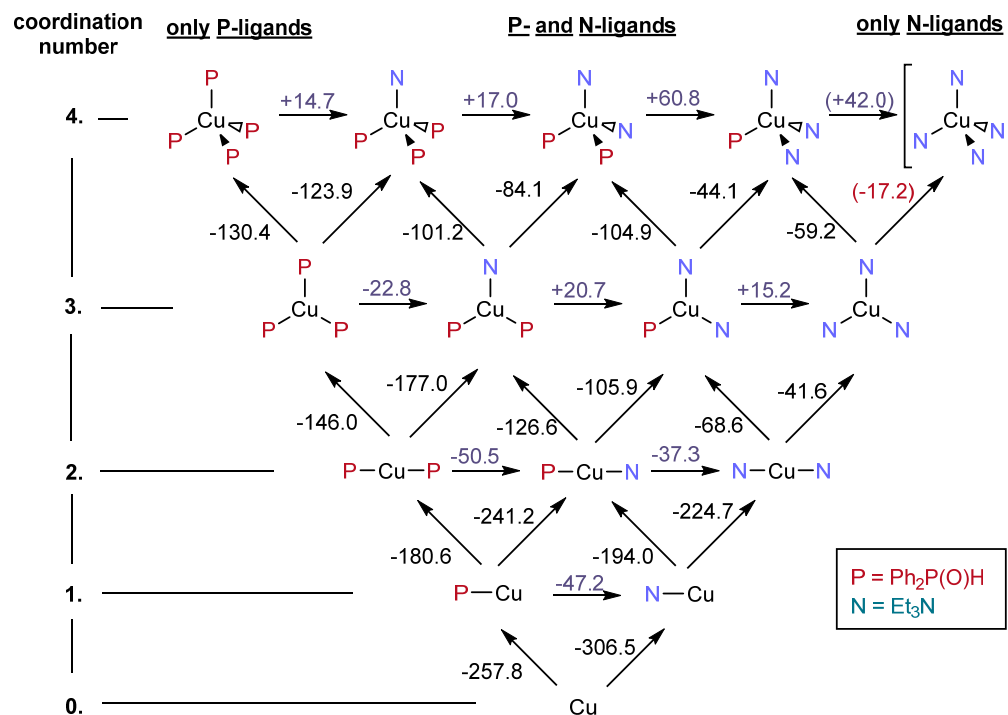


Figure 3. Stepwise complexation of Cu^+ with P- and N-ligands. The CuN_4 in the squared bracket is not an existing complex.

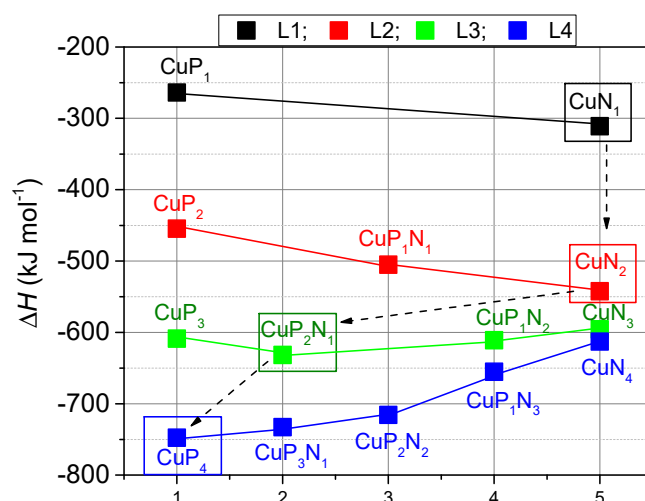


Figure 4. Stepwise mixed complexation of Cu^+ with P- and N-ligands. The species included in a box are the most stable regarding mono-, di-, tri- and tetraligation.

2.4. The Mechanism of the $\text{Cu}(\text{I})$ -Catalyzed Reaction of $\text{Ph}_2\text{P}(\text{O})\text{H}$ with Halogenobenzenes

2.4.1. Assuming Ph_2POH as the Ligand to $\text{Cu}(\text{I})$

Regarding the reaction of $\text{Ph}_2\text{P}(\text{O})\text{H}$ with PhX ($\text{X} = \text{Br}$ or I), in the first approach, the mechanism was modelled assuming the excess of Ph_2POH as the ligand to Cu^+ ion. The bis-coordinated $\text{Cu}(\text{I})$ complex was expected to be the most reactive species. In the first step, the most stable “ $\text{Cu}(\text{I})\text{P}_4$ ” gets decomposed to precatalyst $\text{P-Cu}(\text{I})-\text{P}$ (4) that is

then involved in a series of reaction sequences. The first step is the deprotonation by NET_3 followed by rearrangement to complex $[\text{HOPh}_2\text{P}-\text{Cu}^+-\text{OPPh}_2]$ **4'** that is followed by the interaction of species **4'** with PhX to afford complex **5**. Then, the C-X bond of species **5** is cleaved to afford intermediate **6** via **TS5,6**. In this state (**6**), the oxidation number of Cu is formally increased to 3+; therefore, this copper cation may be considered as a strong oxidizing agent. The endothermic oxidation of the Cu^+ ion to Cu^{3+} is covered by the beneficial formation and coordination of the halide anion (X^-). The next step involves the formation of the C-P bond via four membered **TS6,7**, which leads to the loose complex of the final product Ph_3P (**7**). In this step, the Cu^{3+} is reduced back to Cu^+ , meanwhile the P(III) is oxidized to P(V). Finally, the Ph_3PO product (**1**) leaves the Cu^+ complex that takes up another P-ligand and a newer aromatic reagent for the next cycle (Figure 5).

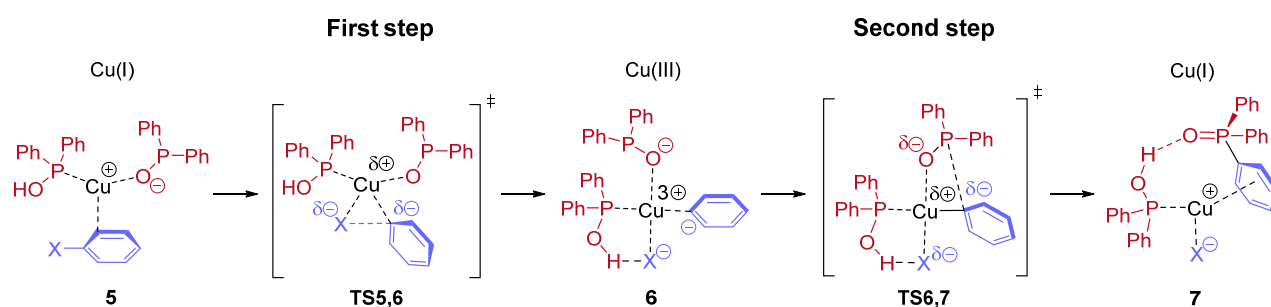


Figure 5. Proposed reaction mechanism (Route I) of the Hirao reaction of $\text{Ph}_2\text{P}(\text{O})\text{H}$ and PhX in the presence of $\text{Cu}(\text{I})(\text{Ph}_2\text{POH})_2$ (**4**).

The energy diagram (Figure 6) for the above transformation (Route I) is shown for the P-C couplings of $\text{Ph}_2\text{P}(\text{O})\text{H}$ with PhI (green line) and PhBr (red line). It can be seen that the energetics for the two instances go parallelly. However, in the last step, in the reductive elimination, the enthalpy level of the final complexes **7** is rather different: for the $\text{X} = \text{I}$ case, it is $-126.7 \text{ kJ mol}^{-1}$, while for the $\text{X} = \text{Br}$ instance, the value is $-320.6 \text{ kJ mol}^{-1}$. Regeneration of the catalyst is more feasible from the iodo containing complex (**7**, $\text{X} = \text{I}$), as this goes with enthalpy gain, as shown in the last step of Figure 6. The sharp difference between the Br^- and I^- may be explained by the stronger and irreversible binding of Br^- to the central Cu^+ ion, as compared to I^- . This may be an explanation for the experience that PhBr cannot be coupled with $\text{Ph}_2\text{P}(\text{O})\text{H}$ in the presence of Cu^+ -catalyst applied in a quantity of 10–20%.

Enthalpy, Gibbs free energy and entropy values belonging to the species involved in Figure 6 are listed in Table 7.

Table 7. Computed reaction enthalpy (ΔH), Gibbs free energy (ΔG) in kJ mol^{-1} and entropy values (ΔS) in $\text{J mol}^{-1}\text{K}^{-1}$ of the Hirao reaction of $\text{Ph}_2\text{P}(\text{O})\text{H}$ and PhX ($\text{X} = \text{Br}$ [red line] and I [green line]) in the presence of $\text{Cu}(\text{I})(\text{Ph}_2\text{POH})_2$ (**4**) in respect to Figure 6.

	X = Br			X = I		
	ΔH (kJ mol^{-1})	ΔG (kJ mol^{-1})	ΔS ($\text{J mol}^{-1}\text{K}^{-1}$)	ΔH (kJ mol^{-1})	ΔG (kJ mol^{-1})	ΔS ($\text{J mol}^{-1}\text{K}^{-1}$)
4	0.0	0.0	0.0	0.0	0.0	0.0
4'	-32.0	-33.2	+3.8	-32.0	-33.2	+3.8
5	-112.8	-68.4	-148.8	-24.0	+25.1	-164.7
TS5,6	-61.4	-9.3	-174.8	40.1	+95.1	-184.7
6	-108.0	-46.8	-205.4	-15.1	+40.3	-188.2
TS6,7	-8.5	+60.0	-229.9	+89.9	+128.4	-129.2
7	-320.6	-269.5	-171.3	-126.7	-84.7	-140.9
1	-65.7	-47.4	-61.3	-176.3	-153.1	-77.9

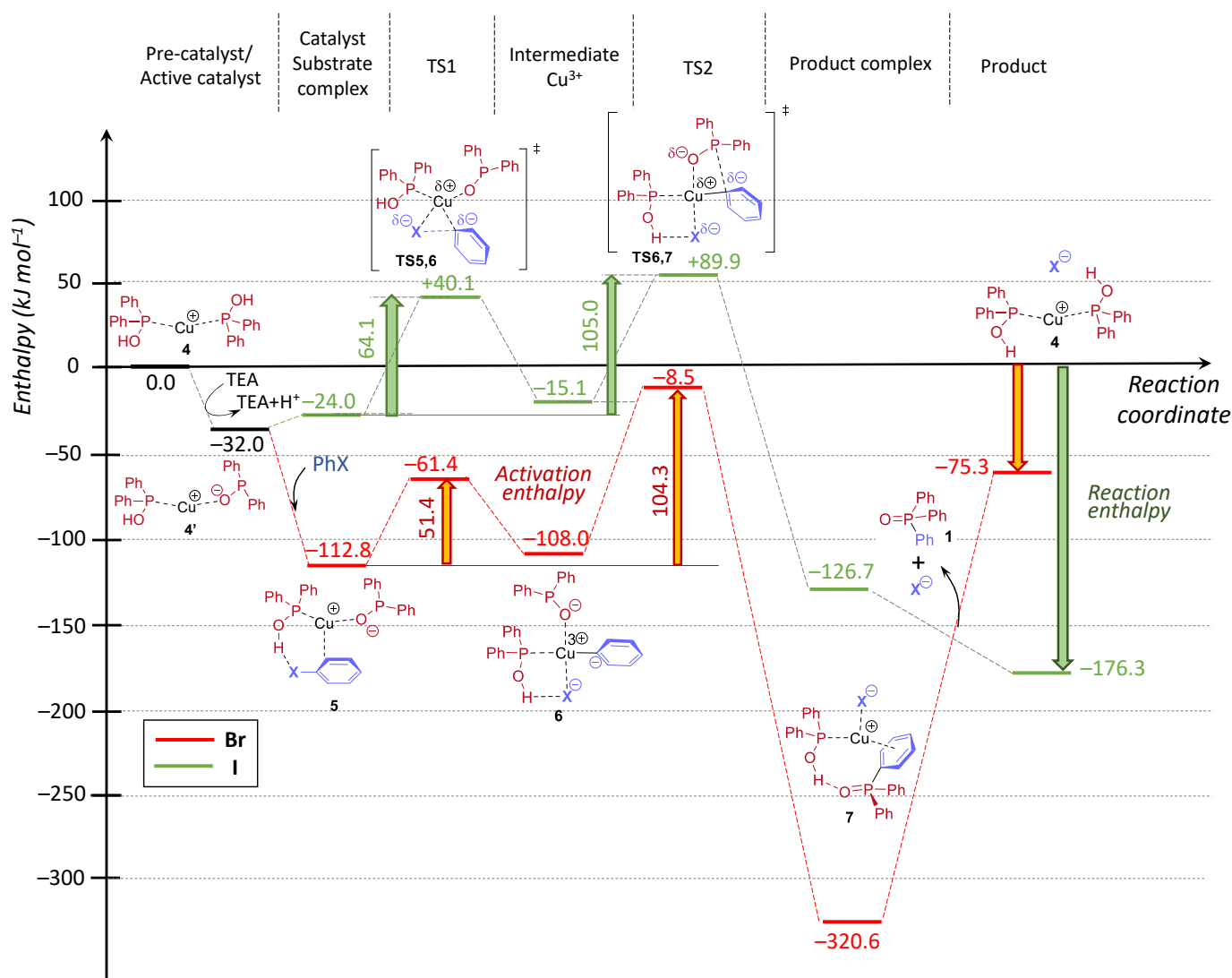


Figure 6. Proposed enthalpy diagram of the Hirao reaction of $\text{Ph}_2\text{P}(\text{O})\text{H}$ and PhX ($\text{X} = \text{Br}$ [red line] and I [green line]) in the presence of $\text{Cu}(\text{I})(\text{Ph}_2\text{POH})_2$ (4).

2.4.2. Assuming Mixed P, N-Ligation and N,N-Ligation of $\text{Cu}(\text{I})$

We also studied the first reaction step (Route I, oxidative addition of the PhBr to the Cu^+ ion) assuming the $\text{P}-\text{Cu}(\text{I})-\text{N}$ (8) and the $\text{N}-\text{Cu}(\text{I})-\text{N}$ (9) complexes as active catalysts (Figure 7). The $\text{P}-\text{Cu}(\text{I})-\text{P}$ (4) species may undergo exchange of one of its P-ligands to TEA that is present in the mixture leading to “mixed” $\text{P}-\text{Cu}(\text{I})-\text{N}$ complex 8. Another replacement may afford $\text{N}-\text{Cu}(\text{I})-\text{N}$ complex 9. The relative enthalpy levels of the three binary $\text{Cu}(\text{I})$ complexes (4, 8 and 9) are shown on the left side of Figure 8, representing that the N-ligation brings the highest stability.

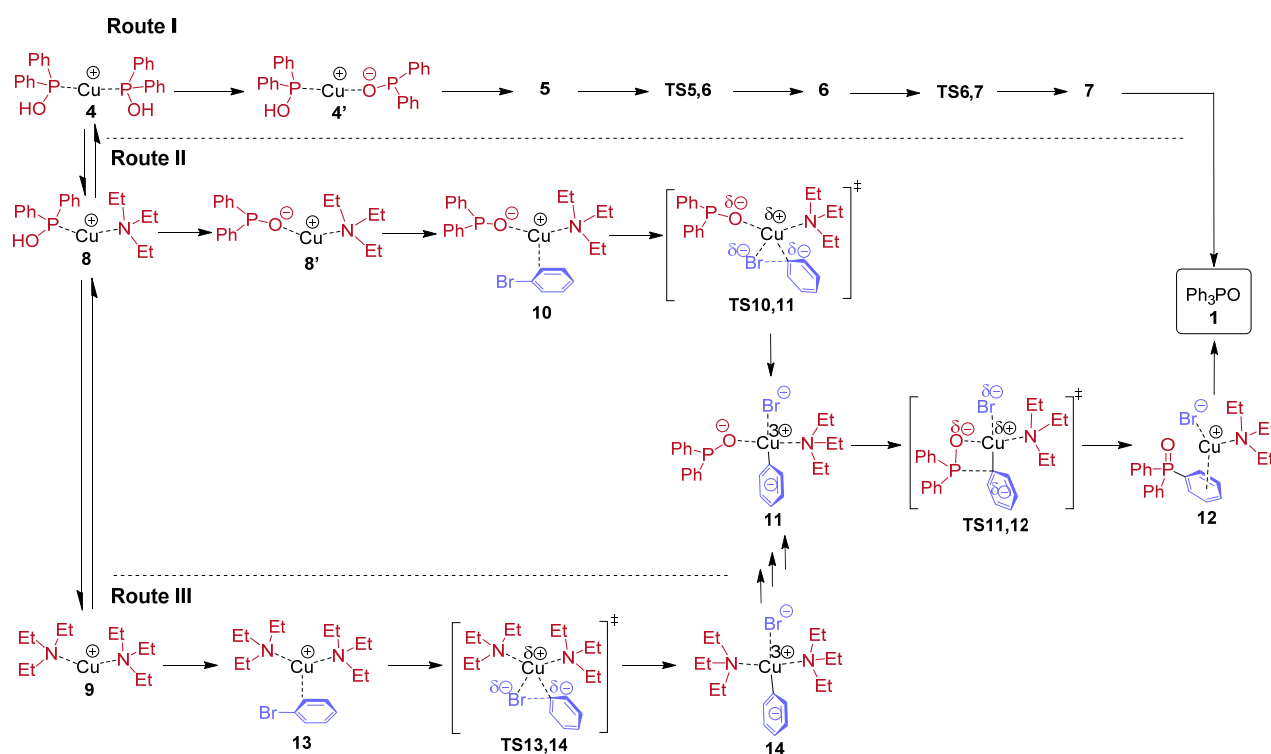


Figure 7. The three possible mechanisms (Route I–III) of the Hirao reaction of $\text{Ph}_2\text{P}(\text{O})\text{H}$ and PhBr in the presence of $\text{Cu}(\text{I})$ complexes with different combination of P- and N-ligands (4, 8 and 9).

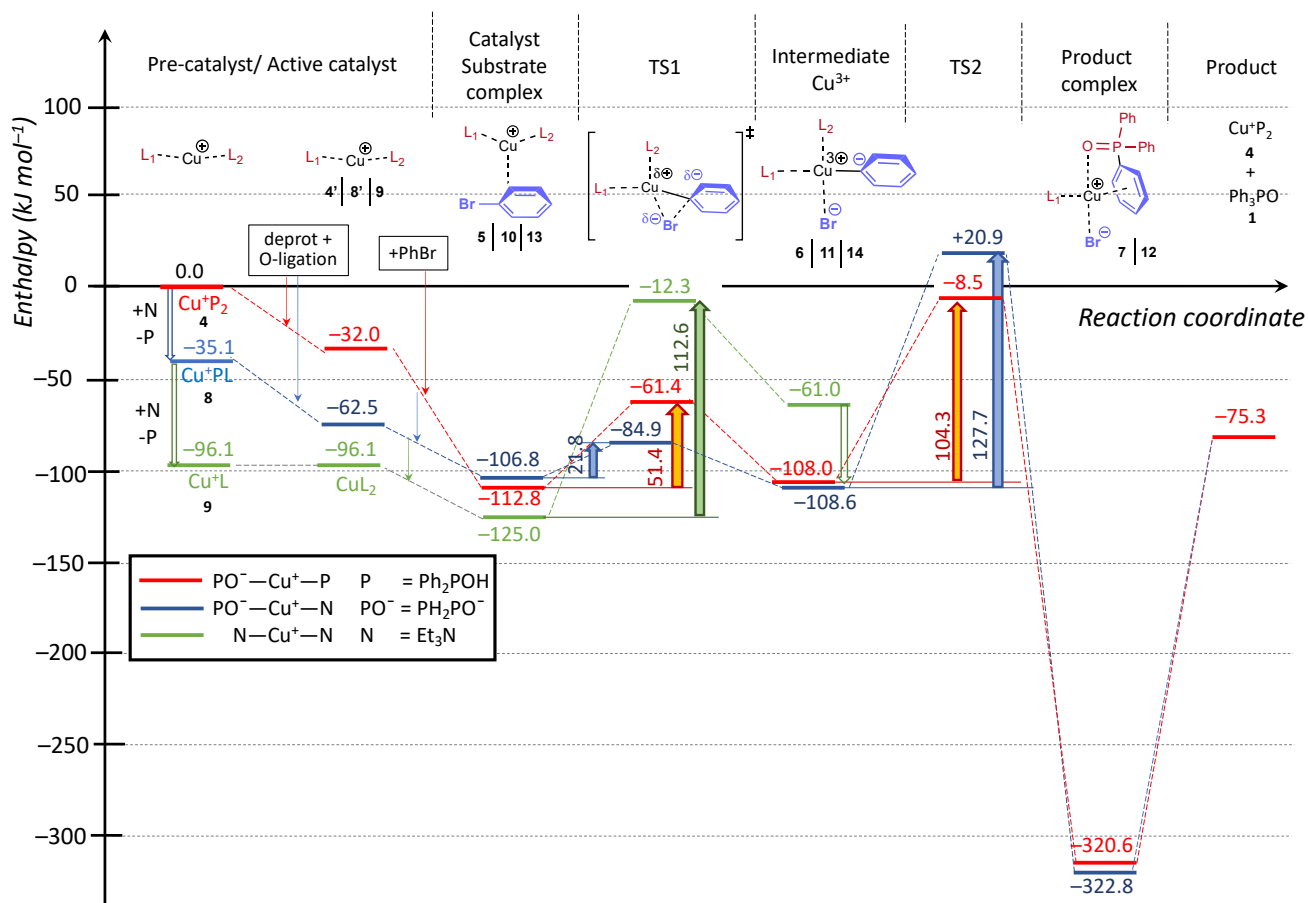


Figure 8. Energetics of the Hirao reaction of $\text{Ph}_2\text{P}(\text{O})\text{H}$ with PhBr assuming different starting complexes.

Enthalpy, Gibbs free energy and entropy values belonging to the additional species shown in Figure 8 are listed in Table 8.

Table 8. Computed reaction enthalpy (ΔH), Gibbs free energy (ΔG) in kJ mol^{-1} and entropy values (ΔS) in $\text{J mol}^{-1}\text{K}^{-1}$ for Route II–III in respect to Figure 8. The values for the diphosphate complex, can be found in Table 7.

	$L_1 = \text{PPh}_2\text{HO}, L_2 = \text{NEt}_3$				$L_1 = L_2 = \text{NEt}_3$		
	ΔH (kJ mol^{-1})	ΔG (kJ mol^{-1})	ΔS ($\text{J mol}^{-1}\text{K}^{-1}$)		ΔH (kJ mol^{-1})	ΔG (kJ mol^{-1})	ΔS ($\text{J mol}^{-1}\text{K}^{-1}$)
4	0.0	0.0	0.0	4	0.0	0.0	0.0
8	−35.1	−36.1	3.4	9	−96.1	−90.0	−20.3
8'	−62.5	−60.1	−8.0	-	-	-	-
10	−106.8	−53.0	−180.5	13	−125.0	−69.0	−187.7
TS10,11	−84.9	−25.9	−198.0	TS13,14	−12.3	45.2	−193.0
11	−108.6	−49.7	−197.3	14	−61.0	0.5	−121.1
TS11,12	+20.9	59.2	−128.5	-	-	-	-
12	−322.8	266.9	−187.6	-	-	-	-
1	−75.3	−49.2	−87.6	-	-	-	-

Species P—Cu(I)—N (**8**) may be involved in an analogous series of reactions as P—Cu(I)—P complex **4** (Figure 7/Route II). This includes a deprotonation and rearrangement to O-ligated complex (**8'**). In the case of P-ligation, the deprotonation by TEA is beneficial, consequently, the deprotonated and then rearranged complexes (**4'** and **8'**) should be considered as the active forms. **8'** then undergoes complexation with PhBr and the species (**10**) so obtained will be the subject of a subsequent oxidative addition to furnish intermediate **11** via **TS10,11**. The next step is the reductive elimination from **11** to afford the loose complex of $\text{Ph}_3\text{P}(\text{O})$ (**12**) via **TS11,12**. The energetics of the transformations under discussion are summarized in Figure 8. One can see that the oxidative addition step involving species **10** goes with a significantly lower activation enthalpy (21.8 kJ mol^{-1}), as compared to that belonging to species **5** of the original route (51.4 kJ mol^{-1}).

As it was mentioned above, the mixed P—Cu(I)—N complex (**8**) may also undergo a P-ligand exchange by a second molecule TEA to furnish N—Cu(I)—N complex (**9**) (Figure 7/Route III). However, the analogous oxidative addition step comprising the **13**→**14** transformation via **TS13,14** involves a rather high enthalpy barrier ($112.6 \text{ kJ mol}^{-1}$) as compared to the previous versions (Figure 8/Route I and II). Hence, this route is not favorable kinetically. At this point, Route III joins Route II after the necessary N→P-ligand exchange, deprotonation and O-ligation, as shown in Figure 8/Route III.

It may be concluded that the involvement of the P—Cu(I)—N complex (**8**) is the most favorable catalyst in Hirao reaction under discussion. Preparative experiments (see Section 2.1) confirmed that the use of two equivalents of the $>\text{P}(\text{O})\text{H}$ reagent (for the catalyst precursor) is harmful, while the application of NEt_3 in an excess is beneficial. This phenomenon may be explained assuming that the complexation of Cu(I) with the tautomeric form of $>\text{P}(\text{O})\text{H}$ ($>\text{POH}$) may proceed until tetraligation that prevents the catalytic process. It is also possible that the complexation of Cu(I) with $>\text{POH}$ is irreversible, or in this case, the ligand exchange is very slow kinetically, while the complexation with NEt_3 is reversible.

Comparing the three analogous reaction mechanisms (Route I–III), one can conclude that the P-containing complexes exhibit significantly lower activation enthalpy in the oxidative addition step, than the bis N-complex. Both the P—Cu(I)—P and P—Cu(I)—N complexes may be relevant, as the activation barriers do not differ significantly. It is noteworthy that the thermodynamic stability of the $\text{Cu}(\text{III})\text{PN}$ and $\text{Cu}(\text{III})\text{P}_2$ complexes at the intermediate state is much lower than that of the $\text{Cu}(\text{III})\text{N}_2$ species. Moreover, the $\text{Cu}(\text{III})\text{N}_2$ complex needs to undergo a ligand exchange (and then a deprotonation and isomeration) to have the phosphine reactant involved. In addition, using PhBr as the starting material, regeneration of the CuL_2 complex is not possible due to the high enthalpy

requirement. Experiments confirmed that PhI is the suitable reactant in the Cu(I)-catalyzed P–C couplings.

As it may be observed in the mechanism (shown in Figure 8), the thermodynamic stability of the central copper ion with different oxidation states (I and III) is significantly influenced by the surrounding ligands. The relative enthalpy for the oxidation process of Cu(I) to Cu(III) strongly decreases with the increase of the number of the P-ligands (0→1→2) in the complex (see Figure 9). Considering the oxidation process Cu(I)→Cu(III), the stepwise exchange of the N-ligands (NEt₃) by a P-ligand goes with decreasing enthalpy differences of 1571.6 kJ mol⁻¹ → 1410.2 kJ mol⁻¹ → 1361.2 kJ mol⁻¹. This unambiguously shows that a P-ligand may bring a higher stability for the Cu(III) oxidation state than the N-ligand. This trend is in contrast with the situation for Cu(I). It means, that the lone electron pair of the P atom may provide a larger electron density for Cu(III) than the N atom. Moreover, this energetic stabilization is not linear, as the first N→P ligand exchange results in a more significant gain (56.6 kJ mol⁻¹) as compared to that assumed for the linear correlation (see red dot and the arrow in Figure 9). In other words, the N→P ligand exchange is exothermic for Cu(I), but endothermic for Cu(III).

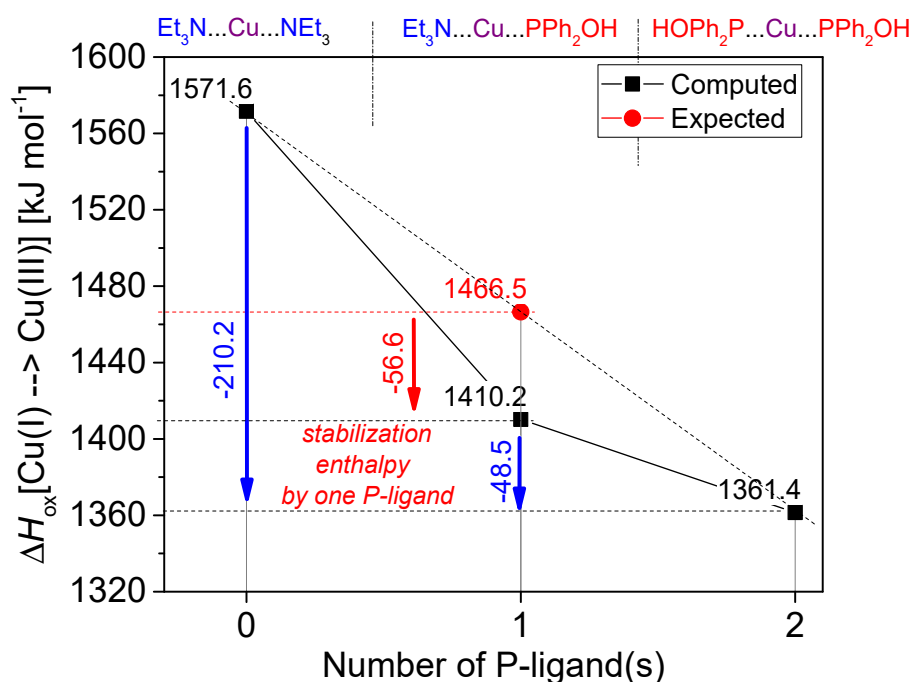


Figure 9. Dependence of the enthalpy difference (ΔH_{ox}) of the Cu(I)L₂ → Cu(III)L₂ transition on the ligands (N = NEt₃, P = PPh₂OH) connecting to the central copper ion.

3. Experimental

3.1. General Information

The reactions were carried out in a CEM[®] Discover Model SP (300 W) (CEM, Microwave Technology Ltd., Buckingham, UK) focused microwave reactor equipped with a stirrer and a pressure controller using 80–100 W irradiation under isothermal conditions. The reaction mixtures were irradiated in sealed borosilicate glass vessels (with a volume of 10 mL) available from the supplier of CEM[®]. The reaction temperature was monitored by an external IR sensor.

The ³¹P, ¹³C and ¹H NMR spectra were taken in CDCl₃ solution on a Bruker AV-300 spectrometer (Bruker Corp., Billerica, MA, USA) operating at 121.5, 75.5 and 300 MHz, respectively. The ³¹P chemical shifts are referred to H₃PO₄, while the ¹³C and ¹H chemical shifts are referred to TMS. The couplings are given in Hz. The exact mass measurements were performed using an Agilent 6545 Q-TOF mass spectrometer (Agilent, Santa Clara, CA, USA) in high resolution, positive electrospray mode.

3.2. The Best Procedures for the P–C Coupling of Iodobenzene and Diphenylphosphine Oxide (Table 1/Entry 9, Table 2/Entries 4 and 8)

To 0.099 mmol of the catalyst (CuI: 0.019 g, CuBr: 0.014 g, CuCl: 0.0098 g) in 1 mL of ethanol were added 0.49 mmol (0.055 mL) of iodobenzene, 0.49 mmol (0.10 g) of diphenylphosphine oxide and 0.99 mmol (0.14 mL) of triethylamine. Then, the resulting mixture was irradiated in a closed vial in the microwave reactor at 165 °C for the times (3 or 4 h) shown in Tables 1 and 2. The reaction mixtures were diluted with 3 mL of EtOH, filtrated and the residue obtained after evaporation was passed through a thin (2–3 cm) layer of silica gel using dichloromethane-methanol 97:3 as the eluent. The crude mixture was analyzed by ^{31}P NMR spectroscopy, then it was purified by column chromatography (silica gel and ethyl acetate–hexane as the eluent).

3.3. The Best Procedures for the P–C Coupling of Iodobenzene and Diarylphosphine Oxides (Table 3/Entries 2, 3, 5 and 6)

To 0.087 mmol of the catalyst (CuCl: 0.0086 g, CuBr: 0.012 g) in 1 mL of ethanol were added 0.048 mL (0.43 mmol) of iodobenzene, 0.43 mmol of diarylphosphine oxide [bis(4-methylphenyl)phosphine oxide: 0.10 g or bis(3,5-dimethylphenyl)phosphine oxide: 0.11 g] and 0.87 mmol (0.12 mL) of triethylamine. Then, the resulting mixture was irradiated in a closed vial in the microwave reactor at 165 °C for 4 h. The reaction mixtures were diluted with 3 mL of EtOH, filtrated and the residue obtained after evaporation was passed through a thin (2–3 cm) layer of silica gel using dichloromethane-methanol 97:3 as the eluent. The crude product was analyzed by ^{31}P NMR spectroscopy, then it was purified by column chromatography (silica gel and ethyl acetate–hexane as the eluent). For the results see Table 3.

3.4. General Procedure for the Competitive Coupling Reaction of Iodobenzene with Diarylphosphine Oxides

To 0.050 mmol (0.0049 g) of copper(I) chloride in 1 mL of ethanol were added 0.50 mmol (0.056 mL) of iodobenzene, 0.25 mmol (0.051 g) of diphenylphosphine oxide, 0.25 mmol of diarylphosphine oxide (bis(4-methylphenyl)phosphine oxide: 0.058 g or bis(3,5-dimethylphenyl)phosphine oxide: 0.065 g) and 0.55 mmol (0.077 mL) of triethylamine. Then, the mixture was irradiated in a closed vial in the microwave reactor at 165 °C for 1.5 h. The reaction mixtures were diluted and filtrated and the residue obtained after concentration was passed through a thin (2–3 cm) layer of silica gel using dichloromethane-methanol 97:3 as the eluent. The crude product was analyzed by ^{31}P NMR spectroscopy. For the results see Table 4.

3.5. Spectral Data for Compounds 1–3 Prepared

3.5.1. Triphenylphosphine Oxide (1)

Appearance: white crystals, ^{31}P NMR (CDCl_3 , 300 MHz) δ 29.1, δ_{P} [29] (CDCl_3 , 162 MHz) 29.5, δ_{P} [8] (CDCl_3 , 121.5 MHz) 30.3; ^{13}C NMR (CDCl_3 , 300 MHz) δ 128.6 (d, $J = 12.1$, C_2)^a, 132.0 (d, $J = 2.8$, C_4), 132.2 (d, $J = 9.9$, C_3)^a, 132.7 (d, $J = 103.8$, C_1), ^amay be reversed, δ_{C} [29] (CDCl_3 , 100 MHz) 128.4 (d, $J = 12.1$), 131.9 (d, $J = 2.2$), 132.5 (d, $J = 9.9$), 132.8 (d, $J = 104.6$); ^1H NMR (CDCl_3 , 300 MHz) δ 7.38–7.48 (m, 6H, ArH), 7.48–7.56 (m, 3H, ArH), 7.59–7.72 (m, 6H, ArH), δ_{H} [29] (CDCl_3 , 400 MHz) δ 7.43–7.48 (m, 6H), 7.52–7.56 (m, 3H), 7.64–7.70 (m, 6H); $[\text{M} + \text{H}]^+ = 279.0934$ $\text{C}_{18}\text{H}_{16}\text{OP}$ requires 279.0939.

3.5.2. Bis(4-methylphenyl)phenylphosphine Oxide (2)

Appearance: white crystals, ^{31}P NMR (CDCl_3 , 300 MHz) δ 27.8, δ_{P} [8] (CDCl_3 , 162 MHz) 29.4, δ_{P} [30] (CDCl_3 , 162 MHz) 30.5; ^{13}C NMR (CDCl_3 , 300 MHz) δ 21.6 (CH_3), 128.5 (d, $J = 12.1$, C_2')^a, 129.3 (d, $J = 12.5$ Hz, C_2)^b, 129.4 (d, $J = 106.6$ Hz, C_1), 131.8 (d, $J = 2.7$ Hz, C_4'), 132.1 (d, $J = 9.8$ Hz, C_3')^a, 132.1 (d, $J = 10.3$ Hz, C_3)^b, 133.1 (d, $J = 104.1$ Hz, C_1'), 142.4 (d, $J = 2.8$ Hz, C_4') ^{a,b}may be reversed, δ_{C} [30] (CDCl_3 , 100 MHz) 21.7, 128.6 (d, $J = 11.8$ Hz), 129.4 (d, $J = 12.6$ Hz), 129.4 (d, $J = 106.9$ Hz), 131.9 (d, $J = 3.2$ Hz), 132.0 (d, $J = 8.7$ Hz), 132.2 (d, $J = 10.2$ Hz), 133.0 (d, $J = 102.5$ Hz), 142.6 (d, $J = 2.9$ Hz); ^1H NMR

(CDCl₃, 300 MHz): δ 2.39 (s, 6H, CH₃), 7.18–7.32 (m, 4H, ArH), 7.37–7.47 (m, 2H, ArH), 7.47–7.61 (m, 5H, ArH), 7.61–7.73 (m, 2H, ArH); δ_{H} [30] (CDCl₃, 400 MHz) 2.38 (s, 6H), 7.24 (dd, $J = 8.4, 2.4$ Hz, 4H), 7.48 (m, 1H), 7.53 (dd, $J = 11.8, 8.0$ Hz, 4H), 7.62–7.68 (m, 2H); $[\text{M} + \text{H}]^+ = 307.1252$ C₂₀H₁₉OP requires 307.1252.

3.5.3. Bis(3,5-dimethylphenyl)phenylphosphine Oxide (3)

Appearance: white crystals, ³¹P NMR (CDCl₃, 300 MHz) δ 29.6, δ_{P} [30] (CDCl₃, 162 MHz) 30.9, ¹³C NMR (CDCl₃, 300 MHz) δ 21.4 (CH₃), 128.4 (d, $J = 12.0$, C_{2'})^a, 129.7 (d, $J = 9.8$, C₂), 131.7 (C_{4'}), 132.1 (d, $J = 9.9$, C_{3'})^a, 132.4 (d, $J = 105.3$, C₁), 133.1 (d, $J = 103.1$, C_{1'}), 133.7 (d, $J = 2.8$, C₄), 138.1 (d, $J = 12.7$, C₃), ^amay be reversed, δ_{C} [30] (CDCl₃, 100 MHz) 21.56, 128.6 (d, $J = 11.7$), 129.8 (d, $J = 10.0$), 131.9 (d, $J = 2.2$), 132.3 (d, $J = 9.7$), 132.4 (d, $J = 102.6$), 133.1 (d, $J = 102.7$), 133.9 (d, $J = 2.3$), 138.3 (d, $J = 12.2$); ¹H NMR (CDCl₃) 2.31 (s, 12H, CH₃), 7.15 (s, 2H, ArH), 7.28 (d, $J = 12.2$, 4H, ArH), 7.39–7.55 (m, 3H, ArH), 7.62–7.73 (m, 2H, ArH), δ_{H} [30] (CDCl₃, 400 MHz) 2.31 (s, 12H), 7.15 (s, 2H), 7.26 (d, $J = 12.4$, 4H), 7.42–7.47 (m, 2H), 7.51–7.55 (m, 1H), 7.63–7.68 (m, 2H); $[\text{M} + \text{H}]^+ = 335.1566$ C₂₂H₂₃OP requires 335.1565.

3.6. Theoretical Calculations

All computations were carried out with the Gaussian16 program package (G16) [31], using standard convergence criteria for the gradients of the root mean square (RMS) Force, Maximum Force, RMS displacement and maximum displacement vectors (3.0×10^{-4} , 4.5×10^{-4} , 1.2×10^{-3} and 1.8×10^{-3}). Computations were carried out at M06-2X level of theory [32]. The basis set of 6-31G(d,p) was applied for C, H, O, P, N, Cl, Br, Cu and SDD/MWB46 for iodine [33]. The vibrational frequencies were computed at the same levels of theory, in order to confirm properly all structures as residing at minima on their potential energy hypersurfaces (PESs). Thermodynamic functions U , H , G and S were computed at 398.15 K. Beside the vacuum calculations, the IEFPCM method was also applied to model the solvent effect, by using the default settings of G16, setting the $\epsilon = 24.852$ [34]. See the Supporting Information for details.

4. Conclusions

The so far less spread and studied Cu(I)-catalyzed Hirao P–C coupling reaction of iodobenzene and diarylphosphine oxides may be best carried out using 20% of CuBr catalyst precursor and two equivalents of triethylamine in ethanol at 165 °C under MW irradiation. The theoretical calculations following a careful study on the P- and N-ligation of Cu(I) proved that the >P(OH)—Cu(I)—NEt₃ “mixed” complex may be the primary catalyst and in the rate determining oxidative addition step, Cu(I) is converted to Cu(III). The “homogeneous” complex P(III)—Cu(I)—P(III) may also be involved in a lesser extent, but the other homogeneous species, Et₃N—Cu(I)—NEt₃ could be excluded on the basis of the energetics. The calculations also suggested that bromobenzene is not a suitable starting material in the P–C couplings investigated. This is the first case that the Cu(I)-catalyzed Hirao reaction was optimized and the mechanism of the P–C coupling was explored.

Supplementary Materials: The following are available online at <https://www.mdpi.com/article/10.3390/catal11080933/s1>, ³¹P, ¹H, and ¹³C NMR spectra of products, energetics and geometrical data belonging to theoretical calculations.

Author Contributions: G.K.: planning, coordinating and supervising the work. Writing the paper and placing the contents into literature context. Fund raising. B.H.: performed the experimental work related. Interpreted the results. R.H.: Critical survey of the literature. Drawing the conclusions. Z.M.: carried out the extensive theoretical calculations related. Drew the conclusions. All authors have read and agreed to the published version of the manuscript.

Funding: This project was supported by the National Research, Development and Innovation Office (K134318).

Conflicts of Interest: The authors declare no conflict of interest.

References

1. Hirao, T.; Masunaga, T.; Ohshiro, Y.; Agawa, T. Stereoselective synthesis of vinylphosphonate. *Tetrahedron Lett.* **1980**, *21*, 3595–3598. [[CrossRef](#)]
2. Hirao, T.; Masunaga, T.; Yamada, N.; Ohshiro, Y.; Agawa, T. Palladium-catalyzed new carbon-phosphorus bond formation. *Bull. Chem. Soc. Jpn.* **1982**, *55*, 909–913. [[CrossRef](#)]
3. Jablonkai, E.; Keglevich, G. Advances and new variations of the Hirao reaction. *Org. Prep. Proced. Int.* **2014**, *46*, 281–316. [[CrossRef](#)]
4. Jablonkai, E.; Keglevich, G. P–C bond formation by coupling reaction utilizing >P(O)H species as the reagents. *Curr. Org. Synth.* **2014**, *11*, 429–453. [[CrossRef](#)]
5. Henyecz, R.; Keglevich, G. New developments on the Hirao reactions, especially from “green” point of view. *Curr. Org. Synth.* **2019**, *16*, 523–545. [[CrossRef](#)]
6. Jablonkai, E.; Keglevich, G. P-Ligand-free, microwave-assisted variation of the Hirao reaction under solvent-free conditions; the P–C coupling reaction of >P(O)H species and bromoarenes. *Tetrahedron Lett.* **2013**, *54*, 4185–4188. [[CrossRef](#)]
7. Keglevich, G.; Jablonkai, E.; Balázs, L.B. A “green” variation of the Hirao reaction: The P–C coupling of diethyl phosphite, alkyl phenyl-*H*-phosphinates and secondary phosphine oxides with bromoarenes using P-ligand-free Pd(OAc)₂ catalyst under microwave and solvent-free conditions. *RSC Adv.* **2014**, *4*, 22808–22816. [[CrossRef](#)]
8. Jablonkai, E.; Balázs, L.B.; Keglevich, G. A P-ligand-free nickel-catalyzed variation of the Hirao reaction under microwave conditions. *Curr. Org. Chem.* **2015**, *19*, 197–202. [[CrossRef](#)]
9. Keglevich, G.; Henyecz, R.; Mucsi, Z.; Kiss, N.Z. The palladium acetate-catalyzed microwave-assisted Hirao reaction without an added phosphorus ligand as a “green” protocol: A quantum chemical study on the mechanism. *Adv. Synth. Catal.* **2017**, *359*, 4322–4331. [[CrossRef](#)]
10. Henyecz, R.; Mucsi, Z.; Keglevich, G. Palladium-catalyzed microwave-assisted Hirao reaction utilizing the excess of the diarylphosphine oxide reagent as the P-ligand; a study on the activity and formation of the “PdP₂” catalyst. *Pure Appl. Chem.* **2019**, *91*, 121–134. [[CrossRef](#)]
11. Henyecz, R.; Mucsi, Z.; Keglevich, G. A surprising mechanism lacking the Ni(0) state during the Ni(II)-catalyzed P–C cross-coupling reaction performed in the absence of a reducing agent—An experimental and a theoretical study. *Pure Appl. Chem.* **2020**, *92*, 493–503. [[CrossRef](#)]
12. Keglevich, G.; Henyecz, R.; Mucsi, Z. Experimental and theoretical study on the “2,2′-bipyridyl-Ni-catalyzed” Hirao reaction of >P(O)H reagents and halobenzenes: A Ni(0) → Ni(II) or a Ni(II) → Ni(IV) mechanism? *J. Org. Chem.* **2020**, *85*, 14486–14495. [[CrossRef](#)]
13. Keglevich, G.; Henyecz, R.; Mucsi, Z. Focusing on the catalysts of the Pd- and Ni-catalyzed Hirao reactions. *Molecules* **2020**, *25*, 3897. [[CrossRef](#)]
14. Gelman, D.; Jiang, L.; Buchwald, S.L. Copper-catalyzed C–P bond construction via direct coupling of secondary phosphines and phosphites with aryl and vinyl halides. *Org. Lett.* **2003**, *5*, 2315–2318. [[CrossRef](#)]
15. Ghalib, M.; Niaz, B.; Jones, P.G.; Heinicke, J.W. σ²-P Ligands: Convenient syntheses of *N*-methyl-1,3-benzazaphospholes. *Tetrahedron Lett.* **2012**, *53*, 5012–5014. [[CrossRef](#)]
16. McDougal, N.T.; Streuff, J.; Mukherjee, H.; Virgil, S.C.; Stoltz, B.M. Rapid synthesis of an electron-deficient *t*-BuPHOX ligand: Cross-coupling of aryl bromides with secondary phosphine oxides. *Tetrahedron Lett.* **2010**, *51*, 5550–5554. [[CrossRef](#)]
17. Craig, R.A.; Stoltz, B.M. Synthesis and exploration of electronically modified (*R*)-5,5-dimethyl-(*p*-CF₃)₃-*i*-PrPHOX in palladium-catalyzed enantio- and diastereoselective allylic alkylation: A practical alternative to (*R*)-(*p*-CF₃)₃-*t*-BuPHOX. *Tetrahedron Lett.* **2015**, *56*, 4670–4673. [[CrossRef](#)] [[PubMed](#)]
18. Karlstedt, N.B.; Beletskaya, I.P. Copper-catalyzed cross-coupling of diethyl phosphonate with aryl iodides. *Russ. J. Org. Chem.* **2011**, *47*, 1011–1014. [[CrossRef](#)]
19. Jiang, D.; Jiang, Q.; Fu, H.; Jiang, Y.; Zhao, Y. Efficient copper-catalyzed coupling of 2-haloacetanilides with phosphine oxides and phosphites under mild conditions. *Synthesis* **2008**, *2008*, 3473–3477. [[CrossRef](#)]
20. Huang, C.; Tang, X.; Fu, H.; Jiang, Y.; Zhao, Y. Proline/pipecolinic acid-promoted copper-catalyzed P-arylation. *J. Org. Chem.* **2006**, *71*, 5020–5022. [[CrossRef](#)]
21. Stankevič, M.; Włodarczyk, A. Efficient copper(I)-catalyzed coupling of secondary phosphine oxides with aryl halides. *Tetrahedron* **2013**, *69*, 73–81. [[CrossRef](#)]
22. Stankevič, M.; Pisklak, J.; Włodarczyk, K. Aryl group—A leaving group in arylphosphine oxides. *Tetrahedron* **2016**, *72*, 810–824. [[CrossRef](#)]
23. Rao, H.; Jin, Y.; Fu, H.; Jiang, Y.; Zhao, Y. A versatile and efficient ligand for copper-catalyzed formation of C–N, C–O, and P–C bonds: Pyrrolidine-2-phosphonic acid phenyl monoester. *Chem. Eur. J.* **2006**, *12*, 3636–3646. [[CrossRef](#)]
24. Zhuang, R.; Xu, J.; Cai, Z.; Tang, G.; Fang, M.; Zhao, Y. Copper-catalyzed C–P bond construction via direct coupling of phenylboronic acids with H-phosphonate diesters. *Org. Lett.* **2011**, *13*, 2110–2113. [[CrossRef](#)]
25. Ogawa, T.; Usuki, N.; Ono, N. A new synthesis of π-electron conjugated phosphonates and phosphonic bis(diethylamides) and their SHG activities. *J. Chem. Soc. Perkin Trans. 1* **1998**, 2953–2958. [[CrossRef](#)]
26. Xiong, B.; Li, M.; Liu, Y.; Zhou, Y.; Zhao, C.; Goto, M.; Yin, S.-F.; Han, L.-B. Stereoselective synthesis of phosphoryl-substituted phenols. *Adv. Synth. Catal.* **2014**, *356*, 781–794. [[CrossRef](#)]

27. Däbritz, F.; Jäger, A.; Bauer, I. Synthesis, Derivatisation and Structural Characterisation of a New Macrobicyclic Phosphane Oxide Cryptand. *Eur. J. Org. Chem.* **2008**, *2008*, 5571–5576. [[CrossRef](#)]
28. Moran, P.H.; Henschke, J.P.; Zanotti-Gerosa, A.; Lennon, I.C. Xyl-TetraPHEMP: A Highly Efficient Biaryl Ligand in the [Diphosphine RuCl₂ Diamine]-Catalyzed Hydrogenation of Simple Aromatic Ketones. *Catal. Fine Chem. Synth.* **2007**, *5*, 101–113.
29. Zhang, X.; Liu, H.; Hu, X.; Tang, G.; Zhu, J.; Zhao, Y. Ni(II)/Zn Catalyzed Reductive Coupling of Aryl Halides with Diphenylphosphine Oxide in Water. *Org. Lett.* **2011**, *13*, 3478–3481. [[CrossRef](#)] [[PubMed](#)]
30. Shen, C.; Yang, G.; Zhang, W. Nickel-catalyzed C–P coupling of aryl mesylates and tosylates with H(O)PR¹R². *Org. Biomol. Chem.* **2012**, *10*, 3500–3505. [[CrossRef](#)]
31. Frisch, M.J.; Trucks, G.W.; Schlegel, H.B.; Scuseria, G.E.; Robb, M.A.; Cheeseman, J.R.; Scalmani, G.; Barone, V.; Petersson, G.A.; Nakatsuji, H.; et al. *Gaussian 16*; revision C.01; Gaussian, Inc.: Wallingford, CT, USA, 2016.
32. Zhao, Y.; Truhlar, D.G. The M06 suite of density functionals for main group thermochemistry, thermochemical kinetics, noncovalent interactions, excited states, and transition elements: Two new functionals and systematic testing of four M06-class functionals and 12 other functionals. *Theor. Chem. Acc.* **2008**, *120*, 215–241. [[CrossRef](#)]
33. Cao, X.Y.; Dolg, M. Segmented contraction scheme for small-core lanthanide pseudopotential basis sets. *J. Mol. Struct.* **2002**, *581*, 139. [[CrossRef](#)]
34. Tomasi, J.; Mennucci, B.; Cammi, R. Quantum Mechanical Continuum Solvation Models. *Chem. Rev.* **2005**, *105*, 2999–3093. [[CrossRef](#)] [[PubMed](#)]